HHS Public Access

Author manuscript

Chembiochem. Author manuscript; available in PMC 2017 July 15.

Published in final edited form as:

Chembiochem. 2016 July 15; 17(14): 1323–1327. doi:10.1002/cbic.201600230.

Photoactivation of an Acid-Sensitive Ion Channel Associated with Vision and Pain

Oliver S. Shafaat, **Dr. Jay R. Winkler**, **Dr. Harry B. Gray*** **[Prof.]**, and **Dr. Dennis A. Dougherty*** **[Prof.]**

Beckman Institute and Division of Chemistry and Chemical Engineering, The California Institute of Technology, 1200 E. California Avenue, Pasadena, CA, 91125, USA

Abstract

We describe the reversible photoactivation of the acid sensitive ligand-gated ion channel ASIC2a, a mammalian channel found throughout the central and peripheral nervous systems that is associated with vision and pain. We have also shown the activation of GLIC, an acid-sensitive prokaryotic homolog of the nicotinic acetylcholine receptor. Photoactivation was achieved using visible-light irradiation of a newly synthesized water-soluble merocyanine photoacid, **1**, which was designed to remove adverse channel blocking effects of a related system. Activation of ASIC2a and GLIC occurs reversibly, in a benign manner, and only upon irradiation. Further studies using transient absorption spectroscopy have shown that protonation of a colorimetric base occurs rapidly (ca. 100 μs) after excitation of **1**. These results demonstrate that irradiation of **1** can induce rapid, local pH changes that can be used to investigate both biological and chemical proton transfer reactions.

The use of light as a trigger for chemical reactions allows for precise control of both the time and location of the reaction. Spatiotemporal control of biological systems allows for in-depth study of a specific target when and where desired. This technique has been applied to activation/inactivation of neurons [1], control of enzymatic function [2–4], and control of drug release to target specific cells [5]. In the case of optogenetics, the photochemical process commonly occurs through a genetically encoded opsin protein [1,6]. Protein functional control, which often requires covalent modification [7–9], uses chromophores such as azobenzene or nitrobenzyl [10,11]. Employing photochemical triggers in living systems requires water-solubility, activation by visible or near-infrared light, minimal toxicity, and no interaction with the biological system that is being studied.

Biological control over local and global proton concentration (pH) is critical to cellular viability. Enzymatic function [12,13], protein structure [14], and lysosomal function [15,16] are a few examples highlighting the importance of pH for proper cellular function. To this end, it would be of value to develop photochemical proton control systems for use in kinetic investigations of these systems. Traditional photoacids, such as 2-naphthol, suffer from biocompatability issues, low solubility, and nanosecond lifetimes (of the photoinduced

hbgray@caltech.edu and dadoc@caltech.edu.

Supporting information for this article is given via a link at the end of the document.

reduction in pK_a) that are shorter than the timing of many biological transformations that rely on H+ transfer [17,18]. Recently, photoacids have been synthesized based on the merocyanine scaffold (Scheme 1a, **3** and **4**). These photoacids can be used to trigger bulk pH changes that persist for seconds [19,20]. We have found, however, that **3** is not amenable to use with ion channels, and the use of **4** is restricted due to its limited solubility in water. We sought to use this scaffold to produce a water-soluble, biocompatible photoacid that could be used to trigger proton-sensitive biological processes.

Acid sensitive ion channels (ASICs) are cation-selective channels that are found throughout the central and peripheral nervous systems in mammals [21,22]. ASICs are ligand-gated, and respond to an increase in the local proton concentration. Crystal structures of ASICs, solved under a variety of conditions, reveal trimeric stoichiometry and a “hand-like” structure, with several acidic amino acids acting as possible proton binding sites [23–25]. These channels are associated with vision, pain, and sensory transmission [26–32]. Another example of an acid-sensitive ion channel is the Gloeobacter ligand-gated ion channel (GLIC), a pentameric, prokaryotic channel that is highly homologous to the large family of mammalian Cys-loop receptors, typified by the nicotinic acetylcholine receptor.

Here, we describe the synthesis of a sulfonated photoacid, **1**, and show that we can trigger activation of two acid-sensitive ligand-gated ion channels, mammalian ASIC isoform 2a and GLIC. Importantly, we show that **1** and its photoproduct **2** do not interact with these channels, apart from the desired photo-triggered proton delivery. We have also investigated the kinetics of proton transfer from **1**. Importantly, our work establishes **1** as a new spatiotemporal tool for the study of pH-sensitive biological and chemical systems.

ASIC2a was expressed heterologously in *Xenopus laevis* oocytes according to literature protocols [33,34]. ASIC activation was monitored using whole-cell voltage-clamp electrophysiology, and expression was verified using pH jumps, with the observed pH_{50} of 3.8, in accord with published data. As a demonstration of photoactivation (Figure 1a), **1**, dissolved in ND96 salts (96 mM aqueous NaCl, 2 mM KCl, 1 mM $MgCl_2$), was pH adjusted to ~5.8, and applied to oocytes expressing ASIC2a. Application of **1** in the dark resulted in a small current change, which is due to the small basal response of ASIC2a to pH 5.8 solutions. After an incubation time of *ca.* 25 s, a 455 nm LED was then used to irradiate a single oocyte. Irradiation occurred for 10 s, which resulted in a rapid rise in current (Figure 1a, black line). This current change is associated with the activation of ASIC2a as a result of the light-activated release of protons by **1** (Scheme 1c). After the LED was turned off, current from ASIC2a returned to baseline. Before and after exposure to **1**, pH 5.5 current response of ASIC2a-expressing oocytes was measured (Figure 1a, red and blue lines respectively). This current response did not change after exposure to **1**, showing that the photoacid does not have any prolonged effect on the channel. Importantly, no current response was observed without irradiation (Figure SI 3a).

This irradiation requirement demonstrates the ability of temporal and spatial activation of ASIC2a with **1**, as both when and where light is delivered are easily tunable. Oocytes not expressing ASIC2a did not show a response upon application or irradiation of **1** (Figure SI 3b). This result shows that native oocyte ion channels are not activated, and the current

response of ASIC2a expressing oocytes under irradiation is attributed to the presence of ASIC2a channels.

When considering the use of photoactive molecules in a biological context, it is crucial to evaluate the effect of both the “pro-drug” (pre-photolysis) as well as the “post-drug” (post-photolysis products) on the system of interest. In the present system, that means that both **1** and **2** cannot interact with the ion channel. To address this concern, **1** was dissolved in pH 5.5 buffer and applied to ASIC2a-expressing oocytes (Figure 1b). The currents observed with **1** in buffer (Figure 1b, black line) are consistent with the pH 5.5 response of ASIC2a to just a buffered solution before application of **1** (Figure 1b, red line). This result indicates that the pro-drug does not deleteriously affect ASIC2a channels. Upon irradiation of this oocyte, no change in current was observed (Figure 1b, black line). Irradiation under these conditions will form **2**, the post-drug; however, a bulk pH change is not induced due to the buffer, allowing an interaction between ASIC2a and **2** to be observed directly. Given that there was no change in current upon irradiation in buffered solution, we conclude that **1** and **2** do not interact deleteriously with ASIC2a.

We have also demonstrated the photoactivation of GLIC, an acid-sensitive member of the pentameric ligand-gated ion channel family. Again, **1** was able to activate GLIC only upon irradiation (Figure 2a), and no deleterious interactions were observed between GLIC and either **1** or **2** (Figure 2b). This establishes that **1** is a generic photoacid, capable of activating a range of channels and, by extension, other acid-sensitive proteins.

Importantly, comparable studies with the related system **4** were not successful. This is because **4** (pre-photolysis), and the spiropyran photoproduct are generic channel blockers, disrupting the function of both ASIC2a and GLIC (SI Figure 3, c and d). It is not unusual for small molecules such as **4**, with significant hydrophobicity and a cationic center, to plug ion channels, a prototype being the local anesthetic lidocaine. It is for this reason that we added the additional sulfonate to **1**, creating a system that is compatible with ion channels.

Synthesis of **1** (Scheme 1b) was carried out by first heating salicylideneaniline in neat sulfuric acid at 100°C, followed by base-catalyzed deprotection to the sulfonated-salicylaldehyde [35]. The product crystallized as brown needles. Condensation with 2-methyl-1-(3-sulfonatepropyl)-benzothiazolium in ethanol afforded **1** as a bright orange powder. **1** is very soluble in water, DMSO, and DMF, slightly soluble in EtOH and MeOH, and insoluble in acetonitrile, ethyl acetate, and acetone.

We have fully characterized the photochemical and photophysical properties of **1**. First, a 20 μM solution of **1** in ND96 salts was adjusted to a pH of *ca.* 6.0 using NaOH. The resulting orange solution exhibits absorption maxima at 416 and 519 nm (Figure 3, black trace). A pH titration of **1** results in clean conversion between two species and an observed pK_a of *ca.* 6.2 (SI Figure 1); the 416 nm band is assigned to the protonated form of the photoacid, and the 519 nm band to the deprotonated form, consistent with literature data [19,20]. Upon irradiation with a 455 nm LED, these visible bands were lost and new bands at 204, 226, and 276 nm developed within seconds (Figure 3, red trace). We assign these bands to the ring-closed, deprotonated spiropyran **2**. The thermal opening of **2** to **1** was monitored by UV-

visible spectroscopy (Figure 3). Clean isosbestic points are present at 197, 260, and 301 nm, and complete conversion back to **1** over an hour. Irradiation outside of the major absorption range of **1** (632.8 nm, HeNe laser) produced only minimal conversion at pH 6.0 after 140 min and no conversion after 60 min at pH 8.0 (Figure SI 2).

The pH of solutions of **1** (*ca.* 1 mM) in ND96 salts was monitored under 455 nm LED irradiation. The starting pH was 6.0, and upon irradiation the pH of the solution dropped and stabilized at *ca.* 3.6 over the course of 2 min. At this time the solution was colorless, as expected from the absorption spectrum of **2**. Again, irradiation into the electronic absorption bands was required for the photochemical process to occur; no pH change was observed after 2 h of 632.8 nm irradiation. When 455 nm irradiation was stopped, the solution slowly (60 min) regained the initial orange color (the final pH was 5.85). This solution was further cycled in the same manner, resulting in the same net pH changes during and after irradiation. This experiment demonstrates that nearly all the protons available from **1** are released under irradiation, resulting in the decreased pH. The bulk pH change can be modulated by the starting pH, as well as the concentration of photoacid in solution; **1** is soluble to at least 85 mM in water. We note that at high concentrations of **1**, the rate of formation of **2** is limited by the irradiation intensity.

We sought to investigate the rate of proton delivery by **1**. To address this matter, the protonation of a pH sensitive dye, bromocresol green (BCG), was monitored using time-resolved nanosecond transient absorption spectroscopy (Figure 4) [17,36]. **1** was dissolved in ND96 salts (pH *ca.* 6.0) and BCG was added. Deprotonated BCG has an intense absorbance peak centered at 616 nm, which decreases upon protonation [37]. A solution of **1** with BCG was excited with a 455 nm pulse of a nanosecond Nd:YAG laser, and protonation of bromocresol green was observed at 632.8 nm using a HeNe probe laser. Excitation resulted in a decreased absorbance at 632.8 nm (Figure 4, black line), indicative of protonation of BCG. The protonation of BCG by **1** was complete in 1 ms. The transient bleach fit well to a single exponential and results in a time constant of *ca.* 100 microseconds. Upon excitation of either **1** or BCG alone, no transient signal at 632.8 nm was observed (Figure SI 4), confirming the observed transient as protonation of BCG by **1**. The protonation kinetics of BCG were examined using two other previously established merocyanine photoacids (**3** and **4**) [19,20]. The concentrations of **1**, **3**, **4** and BCG were equivalent, allowing for the observed protonation rates to reflect the reactivity differences of each photoacid. Replacing the sulfonate with a proton (**4**), and the phenol with an indazole (**3**) resulted in a markedly slower protonation of BCG (Figure 4, blue and red lines, respectively) when compared to **1**.

In summary, we have shown the photoactivation of the acid-sensitive ligand-gated ion channels ASIC2a and GLIC. To the best of our knowledge this is the first report of photoactivation of any acid-sensitive ion channel. Eukaryotic acid-sensitive channels (ASIC) play important roles in stroke, pain, and retinal function.[22,29]. Our approach should be applicable to selective activation of these ASIC channels, allowing for the further study of these channels in complex biological environments. This activation has been achieved through the use of a reversible, highly water-soluble merocyanine photoacid **1**. Proton release from this molecule was triggered by visible light and resulted in a reversible bulk pH change. We have also shown that the protonation of a base was complete within 1 ms. Our

approach allows for the precise spatiotemporal control of proton delivery in aqueous media. The use of this photoacid, and anticipated derivatives with altered pK_a values, is not limited to the activation of ion channels, but can be extended to other physiological and chemical processes associated with proton concentration changes.

Supplementary Material

Refer to Web version on PubMed Central for supplementary material.

Acknowledgments

The authors thank Jeffrey J. Warren for helpful discussions. Professor Stefan Gründer generously provided the ASIC2a plasmid used in this work. Research reported in this publication was supported by The National Institute of Diabetes and Digestive and Kidney Diseases of the National Institutes of Health under award number R01DK019038 to HBG and JRW and by the W. M. Keck Foundation, to DAD. The content is solely the responsibility of the authors and does not necessarily represent the official views of the National Institutes of Health. Additional support was provided by the Arnold and Mabel Beckman Foundation.

References

1. Boyden ES, Zhang F, Bamberg E, Nagel G, Deisseroth K. Nat. Neurosci. 2005; 8:1263–1268. [PubMed: 16116447]
2. Tran N-H, Nguyen D, Dwaraknath S, Mahadevan S, Chavez G, Nguyen A, Dao T, Mullen S, Nguyen T-A, Cheruzel LE. J. Am. Chem. Soc. 2013; 135:14484–14487. [PubMed: 24040992]
3. Roth LE, Nguyen JC, Tezcan FA. J Am Chem Soc. 2010; 132:13672–13674. [PubMed: 20843032]
4. Roth LE, Tezcan FA. J. Am. Chem. Soc. 2012; 134:8416–8419. [PubMed: 22564208]
5. Yavuz MS, Cheng Y, Chen J, Cobley CM, Zhang Q, Rycenga M, Xie J, Kim C, Song KH, Schwartz AG, et al. Nat. Mater. 2009; 8:935–939. [PubMed: 19881498]
6. Deisseroth K. Nat. Neurosci. 2015; 18:1213–1225. [PubMed: 26308982]
7. Lester HA, Krouse ME, Nass MM, Wassermann NH, Erlanger BF. Nature. 1979; 280:509–510. [PubMed: 460432]
8. Lester HA, Krouse ME, Nass MM, Wassermann NH, Erlanger BF. J. Gen. Physiol. 1980; 75:207–232. [PubMed: 6246192]
9. Nomura A, Okamoto A. Chem. Commun. 2009:1906–1908.
10. Kramer RH, Chambers JJ, Trauner D. Nat. Chem. Biol. 2005; 1:360–365. [PubMed: 16370371]
11. Kaplan JH, Forbush B, Hoffman JF. Biochemistry (Mosc.). 1978; 17:1929–1935.
12. Kohse S, Neubauer A, Pazidis A, Lochbrunner S, Kragl U. J. Am. Chem. Soc. 2013; 135:9407–9411. [PubMed: 23688056]
13. Williams JW, Morrison JF. Biochemistry (Mosc.). 1981; 20:6024–6029.
14. Donten ML, Hassan S, Popp A, Halter J, Hauser K, Hamm P. J. Phys. Chem. B. 2015; 119:1425–1432. [PubMed: 25536860]
15. Saftig P, Klumperman J. Nat. Rev. Mol. Cell Biol. 2009; 10:623–635. [PubMed: 19672277]
16. Luzio JP, Pryor PR, Bright NA. Nat. Rev. Mol. Cell Biol. 2007; 8:622–632. [PubMed: 17637737]
17. Gutman M, Huppert D. J. Biochem. Biophys. Methods. 1979; 1:9–19. [PubMed: 45184]
18. Clark JH, Shapiro SL, Campillo AJ, Winn KR. J. Am. Chem. Soc. 1979; 101:746–748.
19. Shi Z, Peng P, Strohecker D, Liao Y. J Am Chem Soc. 2011; 133:14699–14703. [PubMed: 21823603]
20. Abeyrathna N, Liao Y. J. Am. Chem. Soc. 2015; 137:11282–11284. [PubMed: 26305805]
21. Gründer S, Chen X. Int. J. Physiol. Pathophysiol. Pharmacol. 2010; 2:73–94. [PubMed: 21383888]
22. Sherwood TW, Frey EN, Askwith CC. Am. J. Physiol. - Cell Physiol. 2012; 303:C699–C710. [PubMed: 22843794]
23. Baconguis I, Gouaux E. Nature. 2012; 489:400–405. [PubMed: 22842900]

24. Baconguis I, Bohlen CJ, Goehring A, Julius D, Gouaux E. Cell. 2014; 156:717–729. [PubMed: 24507937]
25. Jasti J, Furukawa H, Gonzales EB, Gouaux E. Nature. 2007; 449:316–323. [PubMed: 17882215]
26. Benson CJ, Xie J, Wemmie JA, Price MP, Henss JM, Welsh MJ, Snyder PM. Proc. Natl. Acad. Sci. 2002; 99:2338–2343. [PubMed: 11854527]
27. Bohlen CJ, Chesler AT, Sharif-Naeini R, Medzihradszky KF, Zhou S, King D, Sánchez EE, Burlingame AL, Basbaum AI, Julius D. Nature. 2011; 479:410–414. [PubMed: 22094702]
28. Brockway LM, Zhou Z-H, Bubien JK, Jovov B, Benos DJ, Keyser KT. AJP Cell Physiol. 2002; 283:C126–C134.
29. Deval E, Gasull X, Noël J, Salinas M, Baron A, Diochot S, Lingueglia E. Pharmacol. Ther. 2010; 128:549–558. [PubMed: 20807551]
30. Ettaiche M. J. Neurosci. 2004; 24:1005–1012. [PubMed: 14762118]
31. Ettaiche M, Deval E, Cougnon M, Lazdunski M, Voilley N. J. Neurosci. 2006; 26:5800–5809. [PubMed: 16723538]
32. Ettaiche M, Deval E, Pagnotta S, Lazdunski M, Lingueglia E. Investig. Opthalmology Vis. Sci. 2009; 50:2417.
33. Bartoi T, Augustinowski K, Polleichtner G, Gründer S, Ulbrich MH. Proc. Natl. Acad. Sci. 2014; 111:8281–8286. [PubMed: 24847067]
34. Paukert M, Sidi S, Russell C, Siba M, Wilson SW, Nicolson T, Gründer S. J. Biol. Chem. 2004; 279:18783–18791. [PubMed: 14970195]
35. Driouich R, Takayanagi T, Oshima M, Motomizu S. J. Chromatogr. A. 2001; 934:95–103. [PubMed: 11762768]
36. Nunes RMD, Pineiro M, Arnaut LG. J. Am. Chem. Soc. 2009; 131:9456–9462. [PubMed: 19518094]
37. Lau KT, Shepherd R, Diamond D, Diamond D. Sensors. 2006; 6:848–859.

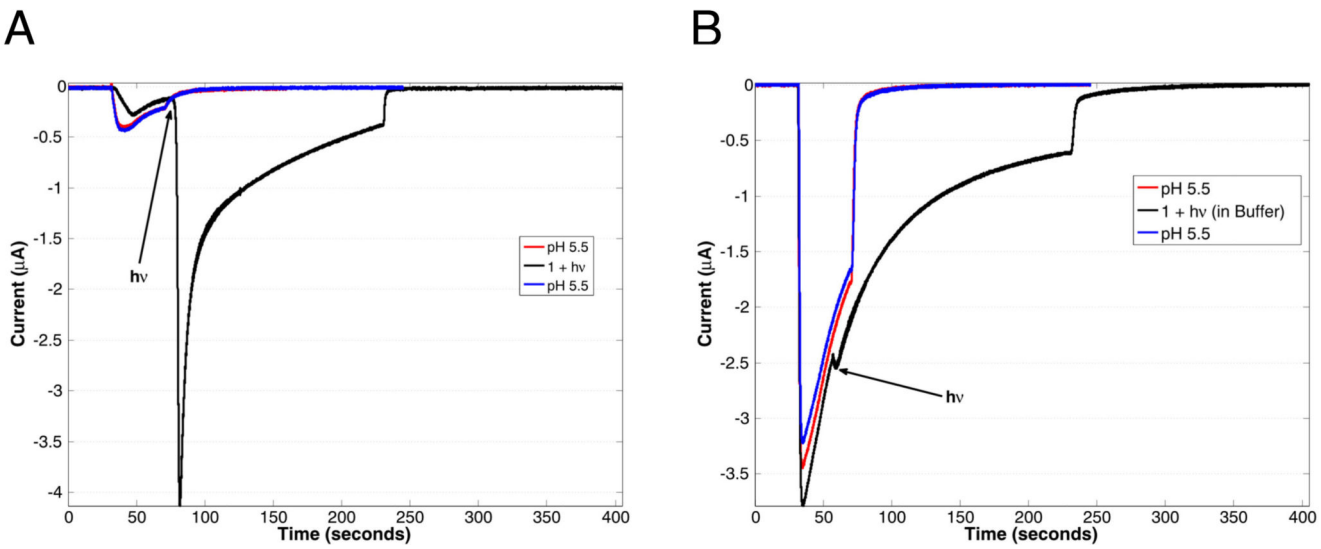

Figure 1.

(A) Activation of ASIC2a upon irradiation (black line, irradiation occurring at position indicated by arrow) for 10 s of 1 (480 uM in pH 5.8 solution) with a 455 nm LED (700 mW peak power), compared to a 30 sec application of a pH 5.5 buffered solution before and after (red and blue lines respectively) application of 1. The much larger current from the photolyzed sample indicates that the local pH is much lower than 5.5, resulting in a larger proportion of open channels. (B) ASIC2a activation in the presence of 1 (280 uM) dissolved in pH 5.5 buffer and irradiated (black line), compared with ASIC2a activation to pH 5.5 buffered solution alone (red and blue lines). The pH 5.5 solutions were washed out after 30 sec, while the sample containing 1 was washed out after 200 sec, with a 10 sec photolysis occurring after 25 sec, as indicated by the arrow. The larger responses to pH 5.5 buffer in panel B simply reflect higher overall expression of the ASIC2a channel in that particular oocyte.

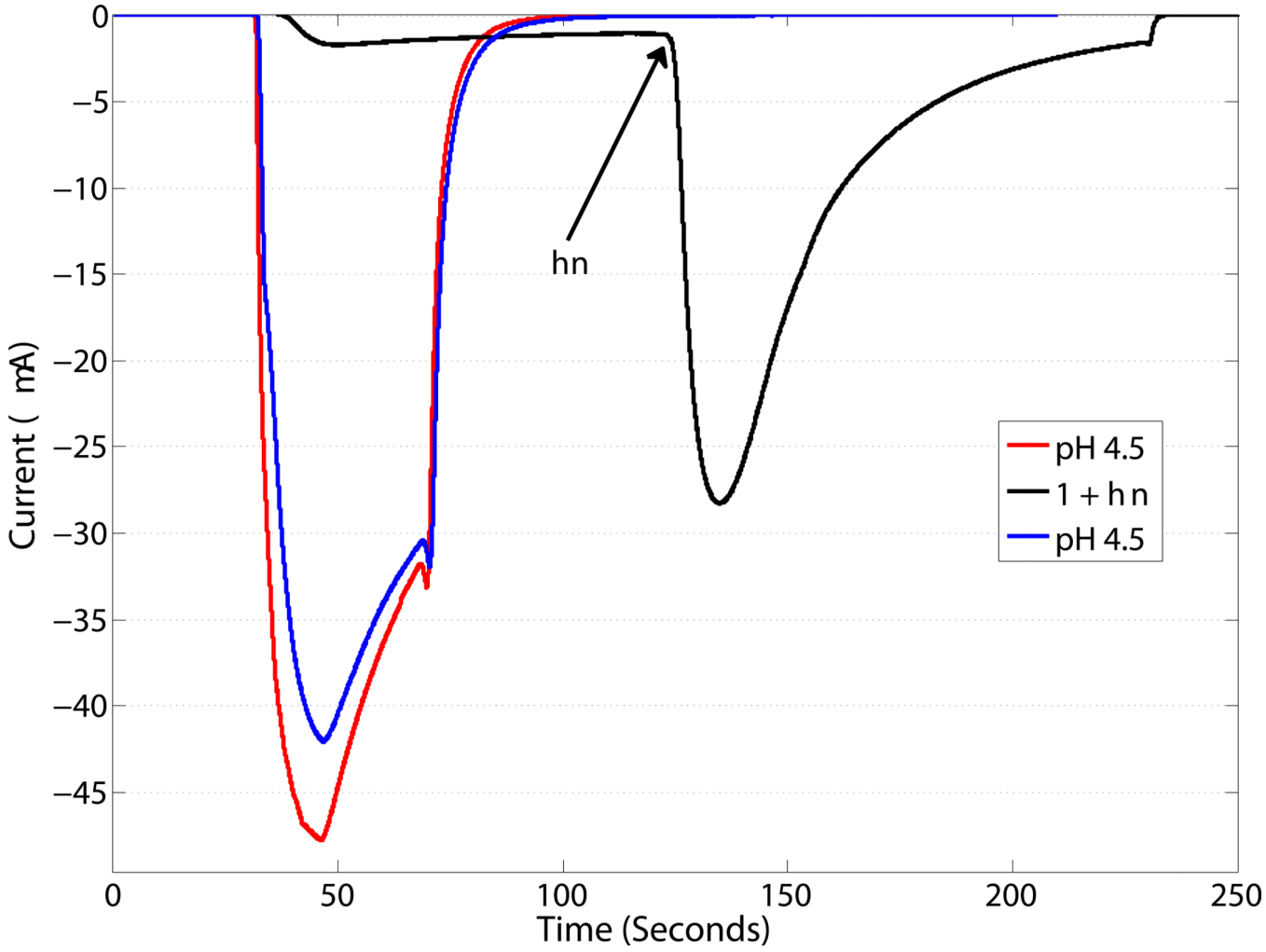

Figure 2.

Activation of GLIC upon irradiation (solid line) for 10 s of **1** (500 uM) with a 455 nm LED (700 mW peak power) compared to a 30 sec application of a pH 4.5 solution (dashed lines) before and after application of **1**.

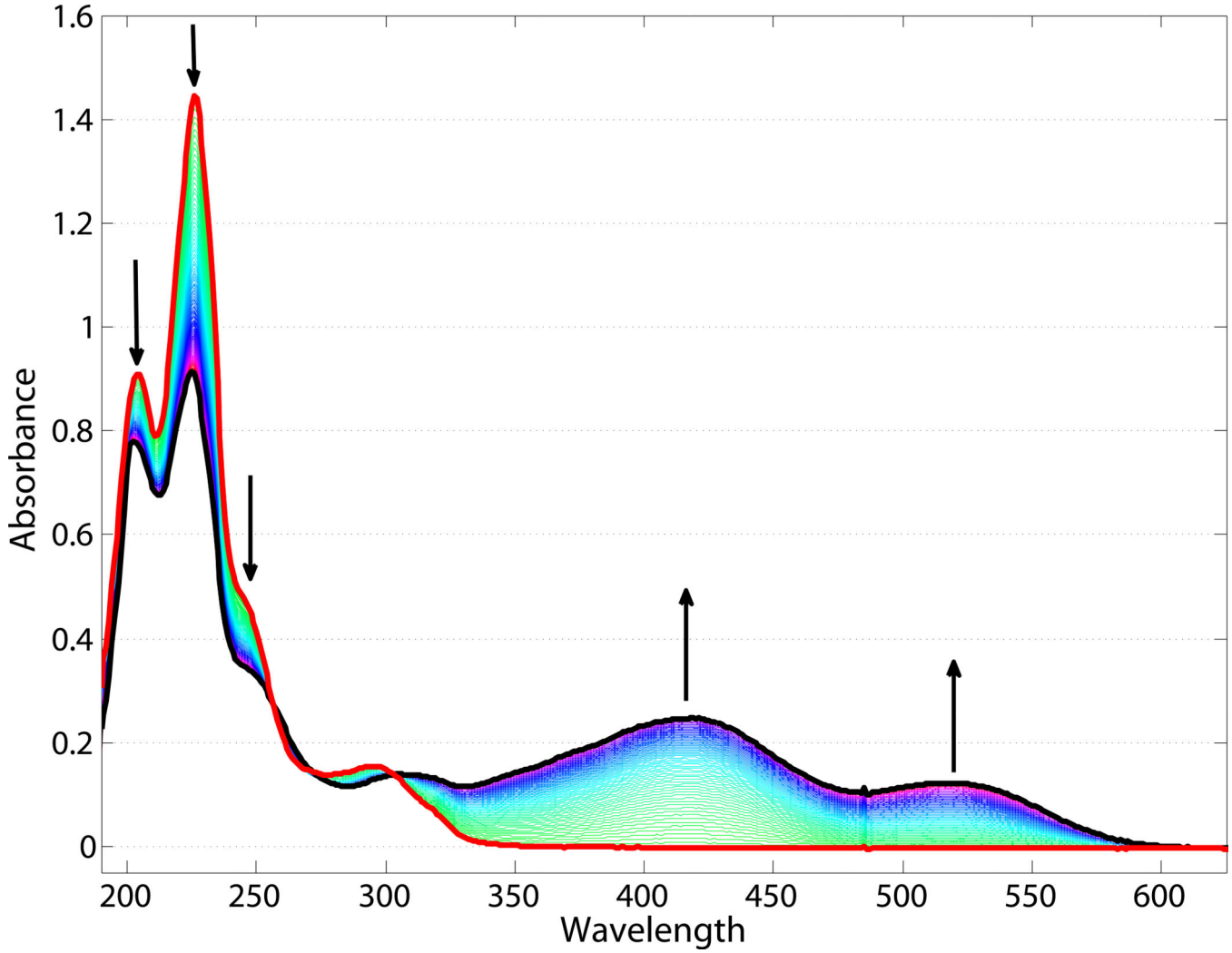

Figure 3.

Electronic absorption spectra of **1** (black trace) in the dark, and **2** (red trace) after irradiation. Arrows indicate changes observed proceeding from **2** to **1** (in the dark) over the course of 75 min.

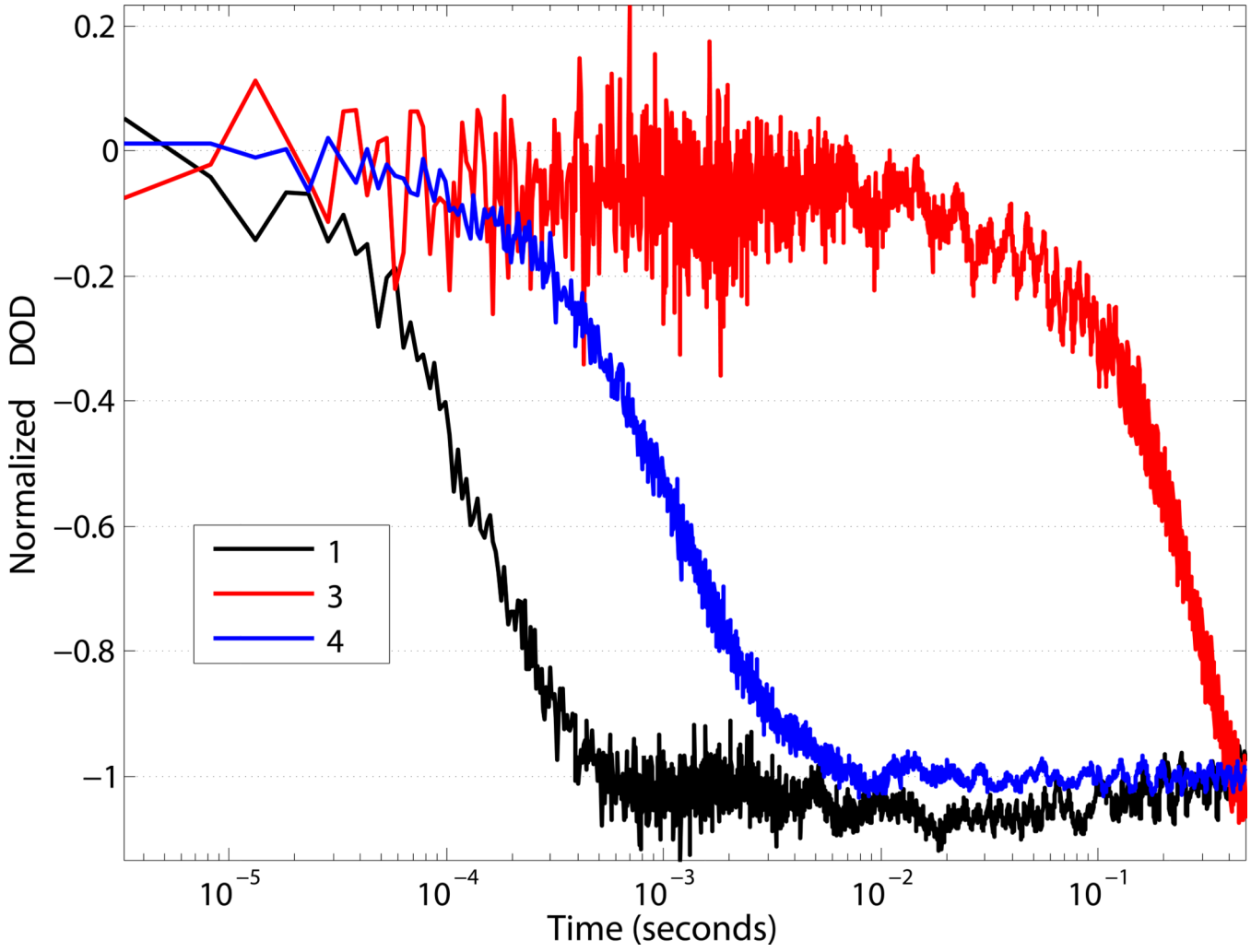

Figure 4.

Normalized single-wavelength transient-absorption at 633 nm monitoring the protonation of bromocresol green (*ca.* 20 μM) by **1**, **3**, and **4** in pH 6.0 water. $\lambda_{excitation}$ = 455 nm.

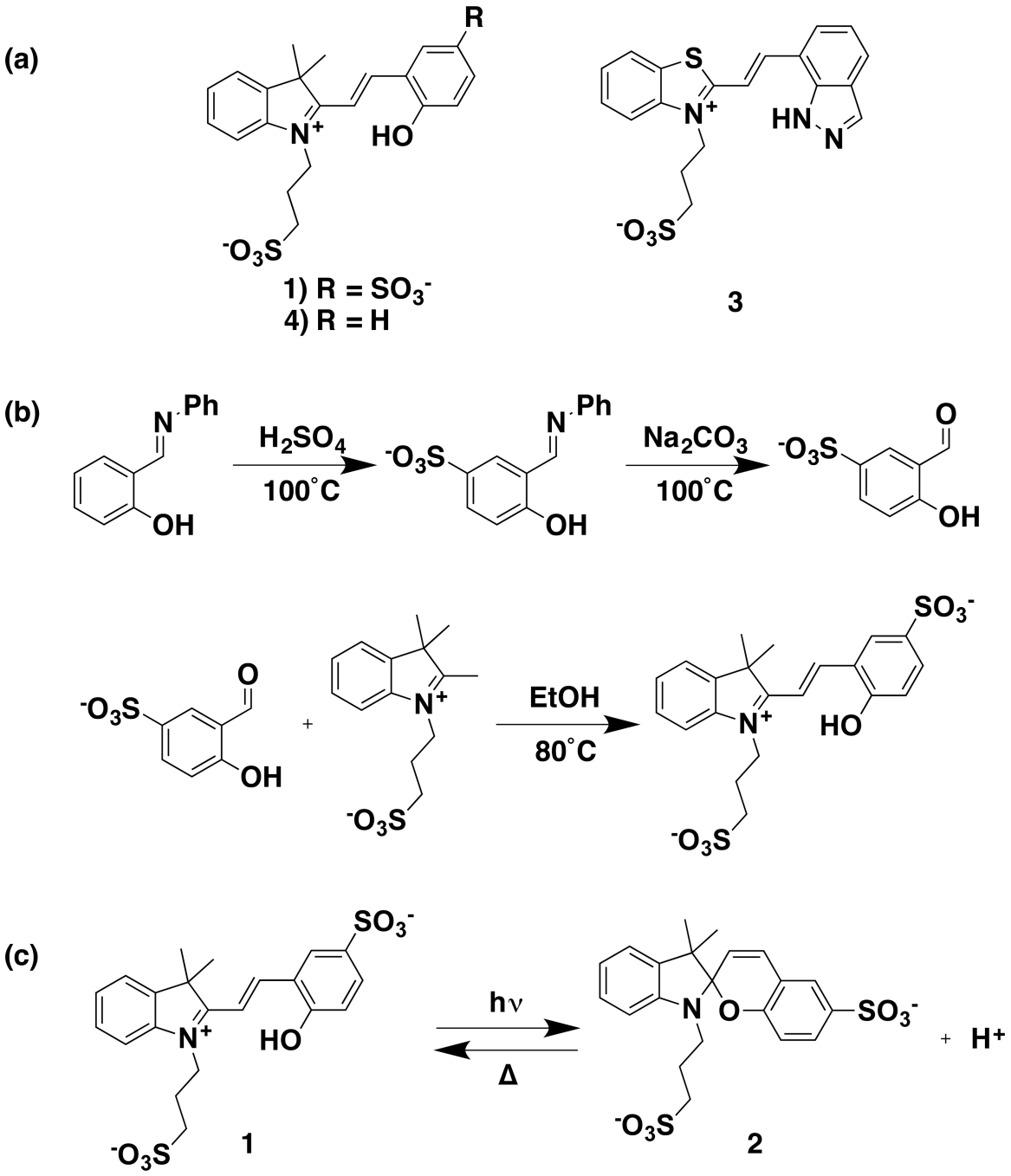

Scheme 1.

(a) Structures of 1, 3, and 4; (b) synthesis of the sulfonated merocyanine photoacid; (c) photoreaction of 1.